2019-11-01

Time-resolved characterization of the mechanisms of toxicity induced by silica and amino-modified polystyrene on alveolar-like macrophages

Deville, S

10.1007/s00204-019-02604-5
Archives of Toxicology
Springer (part of Springer Nature)

Archives of Toxicology (2020) 94:173–186
https://doi.org/10.1007/s00204-019-02604-5

IN VITRO SYSTEMS

Time-resolved characterization of the mechanisms of toxicity induced by silica and amino-modified polystyrene on alveolar-like macrophages

Sarah Deville[1,2,3] · Birgit Honrath[4] · Quynh T. D. Tran[1] · Gyorgy Fejer[5] · Ivo Lambrichts[3] · Inge Nelissen[2] · Amalia M. Dolga[4] · Anna Salvati[1]

Received: 19 June 2019 / Accepted: 23 October 2019 / Published online: 1 November 2019

Abstract

Macrophages play a major role in the removal of foreign materials, including nano-sized materials, such as nanomedicines and other nanoparticles, which they accumulate very efficiently. Because of this, it is recognized that for a safe development of nanotechnologies and nanomedicine, it is essential to investigate potential effects induced by nano-sized materials on macrophages. To this aim, in this work, a recently established model of primary murine alveolar-like macrophages was used to investigate macrophage responses to two well-known nanoparticle models: 50 nm amino-modified polystyrene, known to induce cell death via lysosomal damage and apoptosis in different cell types, and 50 nm silica nanoparticles, which are generally considered non-toxic. Then, a time-resolved study was performed to characterize in detail the response of the macrophages following exposure to the two nanoparticles. As expected, exposure to the amino-modified polystyrene led to cell death, but surprisingly no lysosomal swelling or apoptosis were detected. On the contrary, a peculiar mitochondrial membrane hyperpolarization was observed, accompanied by endoplasmic reticulum stress (ER stress), increased cellular reactive oxygen species (ROS) and changes of metabolic activity, ultimately leading to cell death. Strong toxic responses were observed also after exposure to silica, which included mitochondrial ROS production, mitochondrial depolarization and cell death by apoptosis. Overall, these results showed that exposure to the two nanoparticles led to a very different series of intracellular events, suggesting that the macrophages responded differently to the two nanoparticle models. Similar time-resolved studies are required to characterize the response of macrophages to nanoparticles, as a key parameter in nanosafety assessment.

Keywords Nanoparticles · Nanosafety · Macrophages · Cytotoxicity · Cell death mechanisms

Introduction

Owing to their unique size-related properties, nanoparticles have been proposed as new tools in nanotechnology, including biotechnology and nanomedicine applications (Ferrari 2005; Buzea et al. 2007; Mamo et al. 2010; Blanco et al. 2011; Lobatto et al. 2011; Lam et al. 2018). To ensure a safe development and application of nanotechnologies, their

Electronic supplementary material The online version of this article (https://doi.org/10.1007/s00204-019-02604-5) contains supplementary material, which is available to authorized users.

✉ Anna Salvati
a.salvati@rug.nl

[1] Department Pharmacokinetics, Toxicology and Targeting, Groningen Research Institute of Pharmacy, University of Groningen, A. Deusinglaan 1, 9713 AV Groningen, The Netherlands

[2] Health Department, Flemish Institute for Technological Research, Mol, Belgium

[3] Biomedical Research Institute, Hasselt University, Diepenbeek, Belgium

[4] Department of Molecular Pharmacology, Groningen Research Institute of Pharmacy, University of Groningen, Groningen, The Netherlands

[5] School of Biomedical Sciences, Faculty of Medicine and Dentistry, Plymouth University, Derriford Research Facility, Plymouth, UK

potential effects on cells and organisms need to be evaluated carefully prior to their application (De Jong and Borm 2008; Bouwmeester et al. 2009; Xia et al. 2009; Oberdorster 2010; Rivera Gil et al. 2010; Klein et al. 2011, 2013; Deville et al. 2016).

Within this context, it is recognized that the analysis of cellular responses of macrophages to nanoparticles is a critical parameter for nanosafety assessment (Dobrovolskaia et al. 2008; Lanone et al. 2009; Gustafson et al. 2015; Wiemann et al. 2016; Bhattacharya et al. 2017; Boraschi et al. 2017). Macrophages are, in fact, in the first line of defense against pathogens, including environmental pollution (Figueiredo Borgognoni et al. 2018). They play a major role in the removal of foreign materials by phagocytosis and by mediating inflammatory responses. In this process, macrophages can engulf particulate matter including nanoparticles from the extracellular space very efficiently (Walkey et al. 2012). Indeed, in vivo distribution studies showed that after exposure to nanoparticles, regardless of the exposure route, within the tissues where nanoparticles distribute, macrophages are the cells which usually show the highest nanoparticle accumulation (Pouliquen et al. 1991; Briley-Saebo et al. 2004; Geiser et al. 2008). Similarly in nanomedicine, following intravenous administration, most nanoformulations are known to be rapidly sequestered by macrophages (Owens and Peppas 2006; Walkey et al. 2012), a factor limiting the efficiency of nanoparticle delivery in targeted applications (Wilhelm et al. 2016; Tavares et al. 2017). Additionally, tissue-specific macrophages can respond differently to pathogens and pollution (Gordon et al. 2014; Fejer et al. 2015). Thus, nanoparticles may elicit different toxic responses on the specific resident macrophages within the organs in which they distribute.

Selecting cell models reflecting appropriately the heterogeneity of tissue-specific macrophages is particularly challenging since macrophage models for in vitro studies are affected by several limits (Chanput et al. 2014; Andreu et al. 2017). Macrophages in fact can be best investigated using primary cells. This is because in many cases the genetic background of transformed macrophage cell lines is not well defined, and transformed lines may not reflect well the phenotype of the original macrophage type (Pan et al. 2009; Chanput et al. 2014; Andreu et al. 2017). Nevertheless, given the limited availability of primary macrophages, to have access to sufficient quantities of cells, in vitro studies often use immortalized macrophage cell lines [a classic example being differentiated human THP-1 monocytes (Lunov et al. 2011)], even if they are not always optimal for this purpose.

In the context of nanoparticle-induced toxicity, the lung and its resident phagocytes, the alveolar macrophages, are undoubtedly a relevant model, as the lung constitutes one of the major potential routes of exposure (Schlinkert et al. 2015; Wohlleben et al. 2016; Frijns et al. 2017). Recently, murine Max Planck Institute (MPI) cells have been introduced as novel GM-CSF-dependent, continuously growing, non-transformed macrophages, derived from fetal liver. It has been shown that these cells faithfully reproduce the unique responses of alveolar macrophages, thus they can be used as a rather unique cell model for this type of macrophages (Fejer et al. 2013; Maler et al. 2017; Stichling et al. 2018). Furthermore, unlike to scarcely available alveolar macrophages harvested from bronchoalveolar lavage, this robust system provides unrestricted amounts of primary macrophages for detailed biochemical analysis. Given these unique features, we selected MPI cells to characterize in detail the response of alveolar-like macrophages to two well-characterized nanoparticle types, for which extensive information on the effect on other cell models is already available in literature (Bexiga et al. 2011; Shapero et al. 2011; Lesniak et al. 2012; Wang et al. 2013a, 2018; Ye et al. 2017).

One of the selected nanoparticles were 50 nm amino-modified polystyrene nanoparticles (NH_2-PS), a well-known model to characterize the toxicity induced by (some) positively charged materials (Lv et al. 2006; Aillon et al. 2009; Bexiga et al. 2011; Wang et al. 2013a). While it is known that bare positive charges can cause direct damage to the cell membrane (Ruenraroengsak et al. 2012), once exposed to cells in a more realistic biological environment, NH_2-PS nanoparticles—as most nanomaterials—are covered by proteins and biomolecules. The resulting corona–nanoparticle complexes, usually close to neutrality or slightly negative due to the adsorbed proteins, are then taken up by the cell, where they accumulate in the lysosomes (Bexiga et al. 2011; Wang et al. 2013a, b). Here, the degradation of the original corona protein layer around the nanoparticles can be accompanied by the swelling of the lysosomes and lysosomal rupture, resulting in the release of the lysosomal content into the cytosol and the initiation of apoptosis (Wang et al. 2013a, b). As a second nanoparticle model, 50 nm plain silica nanoparticles (SiO_2) were selected. These are generally well tolerated by cells (Shapero et al. 2011; Lesniak et al. 2012; Ye et al. 2017) and are often considered biocompatible, although some studies suggest that also these nanoparticles can interfere with the physiological cellular behavior (Mohamed et al. 2011) and others indicate that they can elicit inflammatory responses in phagocytes (Park et al. 2011; Kusaka et al. 2014).

A series of assays to measure cellular metabolism, lysosomal alterations, ROS production, mitochondrial processes and apoptosis were combined to determine nanoparticle impact on the alveolar-like macrophages. Thus, a detailed time-resolved analysis on the different end-points selected was performed. The time-resolved approach allowed us to determine the sequence of cellular events following nanoparticle exposure and accumulation in the MPI macrophages

and in this way to characterize their responses to the two nanoparticle models.

Materials and methods

Cell culture

Max Planck Institute (MPI) cells were cultured as previously described in a complete cell culture medium consisting of RPMI 1640 medium (Gibco) supplemented with 10% heat-inactivated fetal bovine serum (FBS, Gibco), 10 µg/ml gentamycin (Gibco) and 20 ng/ml GM-CSF (Peprotech, Bio-Connect, Huissen, Netherlands) (Fejer et al. 2013). For routine sub-culturing, floating and adherent cells harvested with 1.5 mM EDTA (Merck Millipore, Darmstadt, Germany) in phosphate buffer saline (PBS, Gibco, Grant Island, USA) were combined, centrifuged, and resuspended in complete cell culture medium. Cells were seeded at a density of 20,000 cells/cm^2 and subcultured weekly. Cell culture medium was refreshed after 5 days. All experiments were performed with cells between passage 6 and passage 12.

Nanoparticle dispersion preparation, characterization and exposure to cells

MPI cells were exposed to different doses of unlabeled 50 nm plain silica nanoparticles (SiO_2 nanoparticles, Kisker Biotech, Steinfurt, Germany) and 50 nm amino-modified polystyrene nanoparticles (NH_2-PS nanoparticles, Bang Laboratories, Fishers, USA). Nanoparticle dispersions were prepared by diluting the concentrated stock dispersions in complete cell culture medium immediately prior to exposure to the cells. Dispersions were characterized by means of dynamic light scattering and zeta potential determination using a Malvern Zeta Sizer ZS (ZEN 3600, Malvern Instruments, Malvern, UK). Briefly, nanoparticles were diluted to 100 µg/ml in water, PBS and complete cell culture medium and measured at 20 °C immediately after dispersion or after 24 h of incubation at 37 °C and 5% CO_2. Each sample was measured for a total of three measurements which contained each ten runs of 10 s. For each condition, three independent replicate dispersions were prepared and measured. The results are the mean and standard error of the mean (± SEM) of the results obtained from three independent dispersions. Cells were exposed to the nanoparticles by replacing the medium with the freshly prepared nanoparticle dispersions in complete cell culture medium.

Flow cytometry assays on cellular functions

250,000 MPI cells were seeded in a 12-well plate and 48 h after seeding were exposed to different doses of SiO_2 nanoparticles and NH_2-PS nanoparticles in complete cell culture medium for the indicated times. Thereafter, floating and adhering cells harvested with 1.5 mM EDTA in PBS were combined and stained with various fluorescent markers. After staining, cells were washed two times by centrifugation and resuspended in PBS and cell fluorescence intensity was measured immediately using a CytoFLEX flow cytometer (Beckman Coulter, Brea, USA). LysoTracker Red, H_2DCFDA, MitoSOX Red, BODIPY 581/591 Ceraminde-11, TMRE, rhodamine-2 AM, Pacific Blue Annexin V/SYTOX AADvanced were used according to the manufacturer's guidelines (see Supporting Information for detailed information). For all assays, gates in the forward and side scattering double scatter plots were set to exclude cell debris. Cell doublets were excluded in the FSC-A versus FSC-H double scatter plots. A minimum of 20,000 cells were measured (unless specified). Then, the mean of the obtained fluorescence intensity distributions was calculated and the results were normalized by the mean fluorescence intensity of untreated cells. Every experiment was repeated at least two times to confirm the outcomes. The results of individual technical replicates of a representative experiment are shown together with their average.

Measurement of cell viability and caspase 3/7 activity

To assess the viability and caspase 3/7 activation, 25,000 MPI cells were seeded in a 96-well plate and 48 h after seeding were exposed as described above to different doses of SiO_2 and NH_2-PS nanoparticles in complete cell culture medium for the indicated times (100 µl). After the desired exposure time, the medium containing the nanoparticle dispersion was removed and the metabolic activity and caspase activity were measured with, respectively, a MTT (3-(4,5-dimethylthiazol-2-yl)-2,5-diphenyltetrazolium bromide) assay and a Caspase 3/7-Glo kit (Promega, Madison, USA). Detailed protocols are found in the Supporting Information.

Quantitative real-time PCR (qPCR)

For qPCR, 500 000 MPI cells were seeded in a 6-well plate and 48 h after seeding, were exposed to different doses of nanoparticles as described above. Then, total RNA was extracted using Trizol RNA extraction (TRI Reagent Solution, Applied Biosystems, Landsmeer, Netherlands) and cDNA was synthesized from 1000 ng RNA using the Reverse Transcriptase System (Promega). qPCR was performed using SYBR Green (Roche Diagnostics, Almere, Netherlands) for CHOP and Beclin-1. Details are found in the Supporting Information.

Results

Nanoparticle characterization

Prior to exposure to cells, the selected NH_2-PS and SiO_2 nanoparticles (nominal diameter of 50 nm) were characterized using dynamic light scattering and zeta potential measurements to determine their size distribution, stability and surface characteristics in water, PBS and under exposure conditions (Table 1). Overall the results confirmed that exposure to cell culture medium with serum led to biomolecule adsorption and corona formation, as reported for the same nanoparticles in similar studies (Kim et al. 2011; Shapero et al. 2011; Wang et al. 2013a, b, 2018). Importantly, characterization of the dispersions after 24 h incubation in the conditions used for cellular studies confirmed that the nanoparticle dispersions remained stable over the duration of the experiments with cells.

Apoptosis and necrosis after exposure to nanoparticles

As a first step, to investigate how MPI macrophages responded to NH_2-PS and SiO_2 nanoparticles, an Annexin V/SYTOX double staining was used to determine whether cell death was present and eventually to discriminate apoptotic and necrotic cells. Annexin V staining allows to monitor phosphatidylserine appearance on the cell membrane, which is an early sign of apoptosis. SYTOX staining is used to detect an eventual increase in cell membrane permeability, as an indication of cell death (Fig. 1a, b, Supplementary Figure S1). In addition, activation of effector caspases 3/7 upon nanoparticle exposure (Fig. 1c) was also measured. Interestingly, Annexin V/SYTOX staining of cells exposed to NH_2-PS nanoparticles for 24 h showed an increasing number of necrotic cells at increasing doses. Though SYTOX staining does not allow to discriminate primary and secondary necrosis, the absence of clear Annexin V staining at 24 h (also visible in the double scatter plots shown in Supplementary Figure S1) suggested that, as opposed to what is usually observed with these nanoparticles in other cell models (Bexiga et al. 2011; Wang et al. 2013a, b), in MPI macrophages exposure to NH_2-PS nanoparticles led to cell death, but not via apoptosis. This is in agreement with previous observations of necrotic cell death induced by the same nanoparticles in RAW 364.7 macrophages (Hansjosten et al. 2018). On the contrary, SiO_2 nanoparticles displayed a clear apoptotic signature, with both an elevation of the percentage of apoptotic cells and increases in caspase 3/7 activity. Similar results were obtained—again—in RAW 364.7 macrophages (Wilhelmi et al. 2012).

As an additional control, fluorescently labelled variants of similar nanoparticles were used to confirm nanoparticle uptake

Table 1 Nanoparticle characterization by dynamic light scattering and zeta potential measurements

Sample	Medium	Diameter[a] (z-average, nm)	PDI[b]	Diameter[c] (nm)	Zeta potential (mV)
NH_2-PS nanoparticles	0 h in H_2O	56 ± 1	0.08 ± 0.02	–	35 ± 1
	24 h in H_2O	57 ± 1	0.16 ± 0.01	–	28 ± 4
	0 h in PBS	103 ± 7	0.36 ± 0.01	–	18 ± 1
	24 h in PBS	75 ± 17	0.53 ± 0.24	–	24 ± 1
	0 h in CCM	–	–	161 ± 31	− 8 ± 1
	24 h in CCM	–	–	141 ± 25	− 9 ± 1
SiO_2 nanoparticles	0 h in H_2O	69 ± 1	0.28 ± 0.01	–	− 26 ± 1
	24 h in H_2O	68 ± 1	0.18 ± 0.01	–	− 23 ± 1
	0 h in PBS	83 ± 1	0.40 ± 0.02	–	− 14 ± 1
	24 h in PBS	54 ± 1	0.23 ± 0.01	–	− 19 ± 3
	0 h in CCM	–	–	101 ± 9	− 9 ± 1
	24 h in CCM	–	–	155 ± 7	− 9 ± 1

Z-average and polydispersity index (PDI) or average hydrodynamic diameter of 100 µg/ml 50 nm NH_2-PS and SiO_2 nanoparticles after dispersion in water, PBS and complete cell culture medium supplemented with serum (CCM) (0 h) and after 24 h of incubation at 37 °C and 5% CO_2 (24 h). Either cumulant or CONTIN analyses were performed for measurements in buffer and CCM, respectively, to account for multimodal peaks which arise in CCM because of co-detection of the excess free proteins in solution. All values are reported as the mean and standard error of the mean (± SEM) of the results obtained from three independent replicate dispersions

[a]z-average hydrodynamic diameter extracted by cumulant analysis of the data

[b]Polydispersity index (PDI) from cumulant fitting of the data

[c]Average hydrodynamic diameter determined from CONTIN size distribution

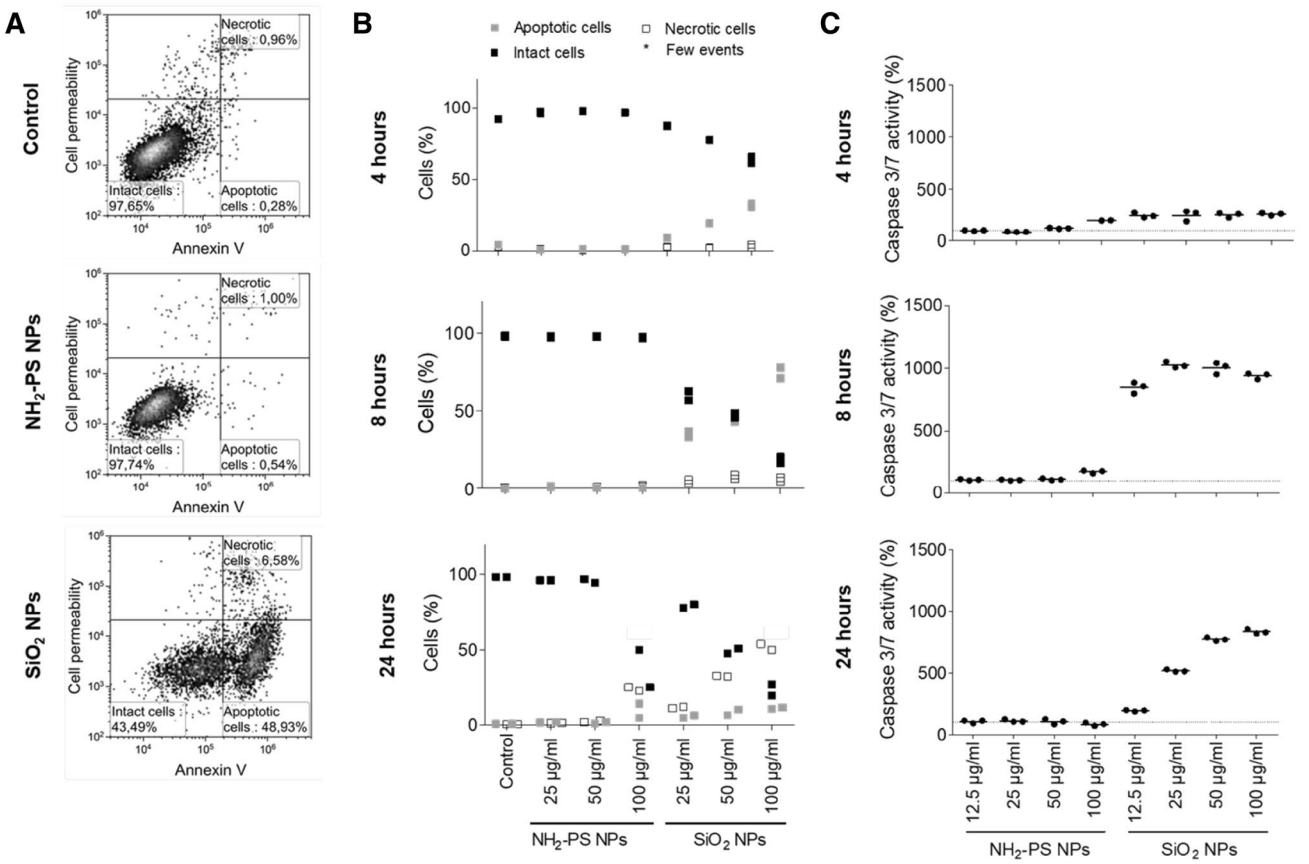

Fig. 1 Activation of cell death in MPI cells exposed to NH_2-PS and SiO_2 nanoparticles. MPI cells were exposed for different times to different doses of nanoparticles, then Annexin V—SYTOX staining was used to monitor eventual presence of apoptotic cells and changes in cell membrane permeability. **a** Representative example of Annexin V—SYTOX double scatter plots after 8 h of exposure. **b** Percentage of intact cells (Annexin V-negative and no increased cell permeability), apoptotic cells (Annexin V-positive cells without increase in cell permeability), necrotic cells (Annexin V-positive cells with increased cell permeability). 20000 cells were measured by flow cytometry (unless indicated) and the percentages in the different gated regions determined (see "Methods" for details). The results of two technical replicates are shown. For cells exposed to 100 µg/ml nanoparticles due to the strong toxicity, it was possible to measure only around 5000 cells (instead of 20000). **c** Activation of the effector caspases 3/7 upon nanoparticle exposure. The results of three technical replicates are shown, together with their mean (indicated with a line), normalized by the results in untreated control cells (dotted line at 100%)

by the MPI cells. Fluorescently labelled COOH-PS were used as an alternative source of polystyrene nanoparticles of comparable size (no fluorescent variant of the NH_2-PS nanoparticles is commercially available). As expected, exposure to 50 nm fluorescently labelled SiO_2 nanoparticles and 40 nm fluorescently labelled carboxylated polystyrene COOH-PS confirmed that nanoparticle uptake in the macrophages was very high (Supplementary Figure S2). We then performed a detailed time-resolved analysis of the mechanisms leading to the observed cell death, to characterize further the differences in the response to the two materials.

Nanoparticle impact on oxidative stress (cellular and mitochondrial ROS levels and lipid peroxidation)

MPI cells were exposed to different concentrations of NH_2-PS and SiO_2 nanoparticles to analyze impact on a series of cellular end-points at different times. Interestingly, flow cytometry analysis showed that cells exposed to SiO_2 nanoparticles displayed clear changes in their forward scatter (FSC, which is related to changes in cell size) and side scatter properties (SSC, which is related to changes in cellular

granularity (e.g. changes in vacuolization) already after only 4 h of exposure. No alterations in forward and side scatter were detected in cells exposed to NH_2-PS nanoparticles (except at the highest dosage and longest exposure time) (Supplementary Figure S3). This alone was already, indicative of a distinct cell response to the two nanoparticle types.

We then examined eventual alterations in cellular ROS levels following exposure to the two nanoparticles. Alterations of ROS levels have often been observed upon exposure to nanoparticles. Some nanoparticles can trigger the direct generation of ROS on their surface (Buzea et al. 2007; Soenen et al. 2011). A part of similar direct ROS production, secondary ROS can also be generated as a consequence of the damage induced by nanoparticles on cell organelles, or via interaction with cell surface receptors and subsequent activation of intracellular signaling cascades (Soenen et al. 2011). Here, cellular ROS production was measured by H_2DCFDA staining (Fig. 2a and Supplementary Figure S4). Already after 4 h of exposure, cellular ROS levels increased in cells exposed to both nanoparticles, while at longer exposure times, they declined to—respectively—moderate and low levels, for cells exposed to, respectively, NH_2-PS and SiO_2 nanoparticles. To determine whether the observed alterations in cellular ROS originated from mitochondrial ROS, cells were labelled with MitoSOX, which specifically measures superoxide production in the mitochondria (Fig. 2b and Supplementary Figure S5). In cells exposed to NH_2-PS nanoparticles, mitochondrial ROS was detected only after 24 h, whereas SiO_2 nanoparticles induced mitochondrial ROS formation already after 4 h of exposure, with a steady increase over the following hours. These findings suggested that NH_2-PS and SiO_2 nanoparticles might have distinct effects on mitochondrial function.

Increased ROS levels can also induce lipid peroxidation in the cell membrane, which in turn can activate pro-apoptotic molecules. Thus, lipid peroxidation was assessed using BODIPY Ceramide-11 staining (Fig. 2c and Supplementary Figure S6). Both NH_2-PS and SiO_2 nanoparticles exhibited a similar increase in lipid peroxidation after 8 and 24 h of exposure.

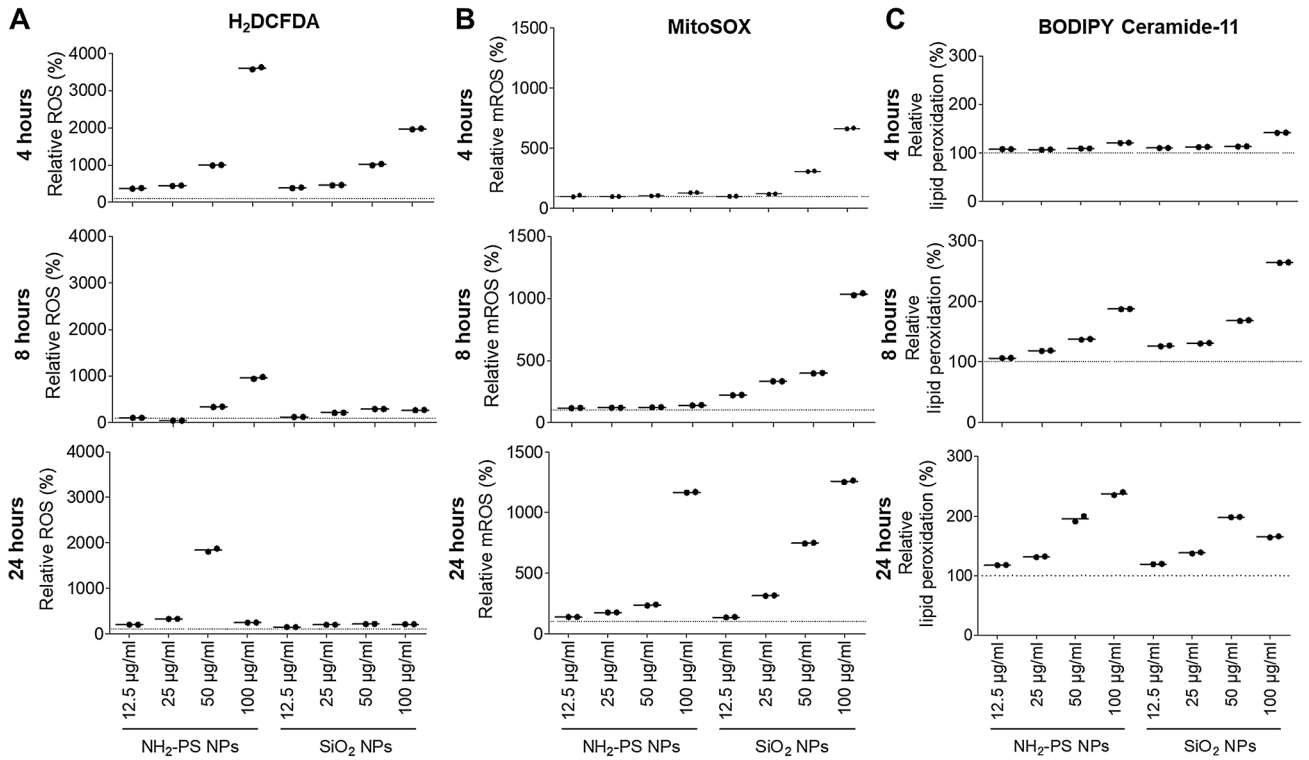

Fig. 2 ROS production and lipid peroxidation in MPI cells after exposure to NH_2-PS and SiO_2 nanoparticles. MPI cells were exposed to different doses of NH_2-PS and SiO_2 nanoparticles for the indicated times, thus cellular ROS (**a**), mitochondrial ROS (**b**) and lipid peroxidation (**c**) were determined, using, respectively, an H_2DCFDA assay, MitoSOX and by BODIPY Ceramide-11 (C11). The results of two technical replicates are shown, together with their mean (indicated with a line), normalized by the results in untreated control cells (dotted line at 100%). Representative examples of the corresponding cell fluorescence intensity distributions are shown in Supplementary Figures S4–6

Nanoparticle impact on mitochondria (metabolic activity, mitochondrial membrane potential and intracellular calcium)

Next, we characterized further nanoparticle impact on mitochondrial functions. Mitochondria play an important role in the regulation of cellular metabolism, apoptosis and immune responses, and are also in close functional contact with other cell organelles involved in the uptake of nanoparticles, such as endosomes and lysosomes (Auten and Davis 2009). Mitochondrial damage is involved in cell death mechanisms such as apoptosis, oxytosis, ferroptosis, necroptosis, among others (Tait and Green 2013; Thornton and Hagberg 2015; Neitemeier et al. 2017). To determine nanoparticle impact on mitochondrial functions, cellular metabolic activity (as measured by the MTT assay), mitochondrial membrane potential and intracellular calcium release were monitored over time. When MPI cells were exposed to NH_2-PS nanoparticles, the cellular metabolic activity declined very fast (Fig. 3a). On the other hand, in cells exposed to SiO_2 nanoparticles, a decreased cellular metabolic activity was observed only after 24 h. The mitochondrial membrane potential was assessed by TMRE (tetramethylrhodamine ethyl ester), a positively charged compound sequestered by the negatively charged mitochondria. Here, a loss in TMRE staining indicates a loss in mitochondrial membrane potential or membrane depolarization. Surprisingly, exposure to NH_2-PS nanoparticles for concentrations up to 50 µg/ml resulted in a steady increase of mitochondrial membrane potential (Fig. 3b and Supplementary Figure S7). On the contrary, for the higher NH_2-PS nanoparticle doses and in cells exposed to the SiO_2 nanoparticles a gradual mitochondrial depolarization was observed over time, as expected when strong cell death is observed. In addition to mitochondrial membrane potential, intracellular calcium levels were also monitored. An increase in intracellular calcium can affect intracellular signaling pathways and trigger cell death (Duchen 2000; Finkel et al. 2015). Staining for intracellular calcium by the calcium indicator rhodamine-2 AM revealed that exposure to both NH_2-PS and SiO_2 nanoparticles induced calcium accumulation. Interestingly, the effect was observed only after 24 and 4 h of exposure, respectively (Fig. 3c and Supplementary Figure S8), time frames consistent with the observed alterations in mitochondrial ROS production (Fig. 2b).

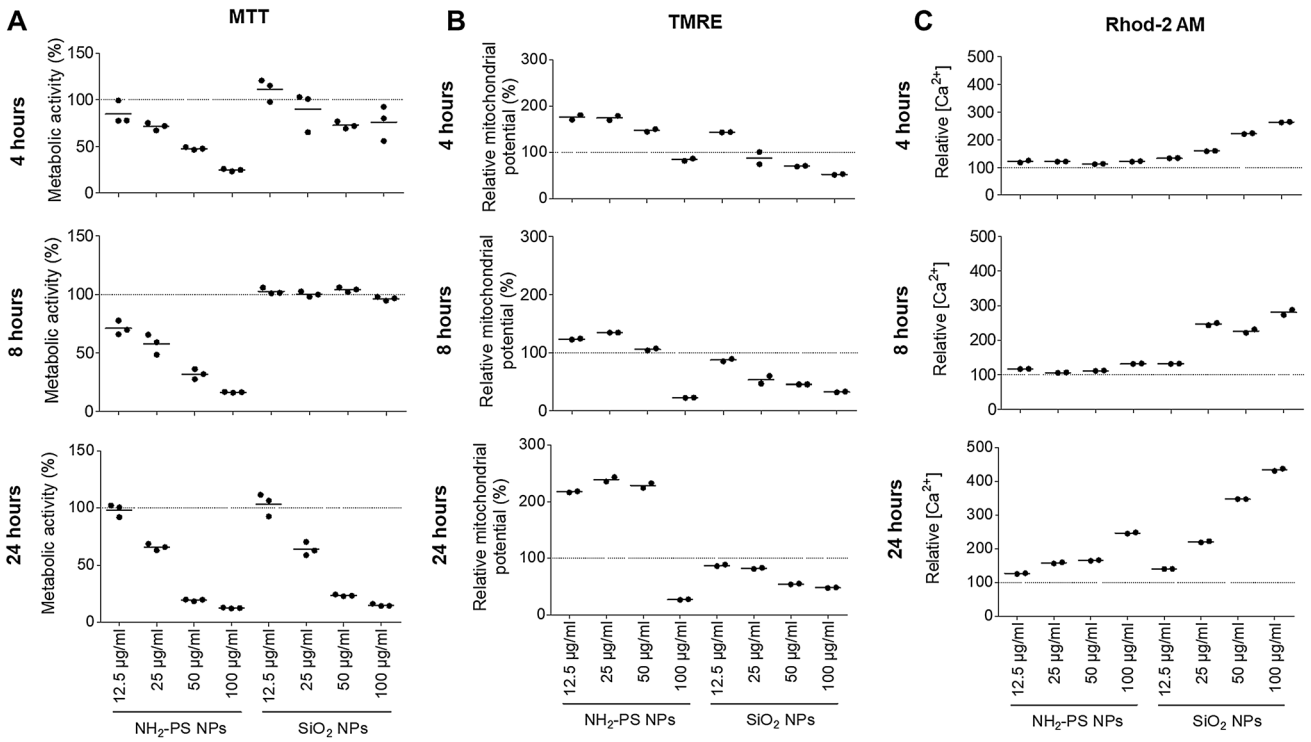

Fig. 3 Effect of NH_2-PS and SiO_2 nanoparticles on mitochondria in MPI cells. MPI cells were exposed to different doses of NH_2-PS and SiO_2 nanoparticles for the indicated times, thus metabolic activity (**a**), mitochondrial membrane potential (**b**) and intracellular calcium levels (**c**) were monitored, respectively, by MTT assay, TMRE staining and with the calcium indicator rhodamine-2 AM. The results of technical replicates are shown together with their mean (indicated with a line), normalized by the results in untreated control cells (dotted line at 100%). Representative examples of the corresponding cell fluorescence intensity distributions are shown in Supplementary Figures S7–8

Nanoparticle impact on lysosomes

As a next step, we investigated whether lysosomal alterations were induced on the macrophages. It has been previously shown that lysosomal alterations play a major role in NH_2-PS nanoparticle-induced cell death in other cell models, with lysosomal swelling, followed by lysosomal rupture and release of the lysosomal content in the cytosol, ultimately activating apoptosis (Wang et al. 2013a, b). Interestingly, on MPI macrophages, LysoTracker staining showed no signs of lysosomal swelling following exposure to NH_2-PS nanoparticles (Fig. 4a, b). No changes in LysoTracker staining were detected also in cells exposed to SiO_2 nanoparticles. Only at the later exposure times, a population with a decrease in LysoTracker Red staining started to appear. Although this result alone does not allow to fully exclude involvement of lysosomal injury in the mechanism of cell death, LysoTracker staining combined with the metabolic activity assays for the same conditions suggests that those cells are most likely dead or dying cells which cannot be stained by LysoTracker. Additionally, no evident sign of lysosomal swelling was observed also via imaging and immunostaining with LAMP1A (a general marker for the lysosomal compartment) (Fig. 4c and Supplementary Figure S9).

Endoplasmic reticulum stress and autophagy

As a final step, we examined potential activation of ER stress and/or autophagy in response to the two nanoparticles, as previously observed with other systems (Cao et al. 2017; Wang et al. 2018). To assess whether ER stress or autophagy were involved, quantitative real-time PCR was performed to measure, respectively, CHOP and beclin-1 expression at different exposure times. CHOP expression in cells is usually low and increases when ER stress is present. High levels of CHOP will eventually result in apoptosis (Cao et al. 2017). Beclin-1 on the other hand is involved in the initiation of autophagy by forming the isolation membrane, which engulfs cytoplasmic components to make the autophagosome. High levels of beclin-1 will also result in the induction of apoptosis (Kang et al. 2011). Interestingly, exposure to NH_2-PS nanoparticles resulted in a strong increase of CHOP expression (Fig. 5a), indicative of ER stress induction. This is particularly surprising as the ER stress-related CHOP expression is commonly associated with the activation of apoptosis which here was not detected (Fig. 1) (Cao et al. 2017). On the contrary, no alteration of CHOP expression was observed in cells exposed to the SiO_2 nanoparticles. Furthermore, no alterations in beclin-1 were observed in cells exposed to the two nanoparticles (Fig. 5b). Similarly, LC3A/LC3B staining of autophagosomes did not show any evident change in cells exposed to the two nanoparticles (Fig. 5c and Supplementary Figure S10). Thus, no clear involvement of autophagy was observed by quantification of beclin-1 expression and LC3 staining.

Discussion

Nanoparticle accumulation in macrophages is commonly observed in the organs where they distribute, making nanoparticle impact on these cells a relevant parameter to be assessed in nanosafety. Given their unique features, including—among others—their high nanoparticle uptake efficiency, macrophages may respond to nanoparticles in different ways than what is usually observed in non-phagocytic cells.

Within this context, in this work, we studied in detail the response of MPI alveolar-like macrophages to two common nanoparticles, namely NH_2-PS and SiO_2 nanoparticles, well-characterized models used in many nanoparticle studies. While the NH_2-PS are a good example to study toxicity induced by positively charged materials, for the SiO_2 nanoparticles ambivalent toxic effects have been reported. In fact, silica nanoparticles are usually considered non-toxic (Bexiga et al. 2011; Shapero et al. 2011; Lesniak et al. 2012; Wang et al. 2013a, b, 2018; Ye et al. 2017). However, other investigations have demonstrated that SiO_2 nanoparticle exposure can hamper cellular functioning (Wiemann et al. 2016; Mohamed et al. 2011; Lankoff et al. 2013; Kim et al. 2015).

While for toxicological studies, the cell-delivered dose should be determined to take into account differences in the way different materials settle on adherent cells (Thomas et al. 2018), our aim here was to detect potential differences in the mechanisms of toxicity induced by the two nanoparticles. To this aim, a range of doses was selected to ensure cytotoxic responses were present, but not too strong, so that clear trends over time could be determined for the different selected endpoints and compared for the two materials. The time-resolved investigation allowed us to highlight unique features in the response of MPI macrophages to these two nanoparticle models.

While NH_2-PS nanoparticle-induced toxicity is usually driven by a strong impact on the lysosomes where the nanoparticles accumulate (Wang et al. 2013a, 2018), our results indicated that these nanoparticles showed a distinct behavior in MPI macrophages, without strong evidence of lysosomal swelling and of apoptosis. However, other investigations have shown the involvement of lysosomal injury in the mechanisms of toxicity induced by these nanoparticles in RAW264.7 macrophages (Xia et al. 2008; Hsia et al. 2019) and the observed loss of LysoTracker Red staining could also be interpreted as a sign of lysosomal malfunctioning, e.g. due to mild lysosomal membrane permeabilization (Wang et al. 2018). Clearly, exposure to NH_2-PS nanoparticles caused a fast increase in cellular ROS production,

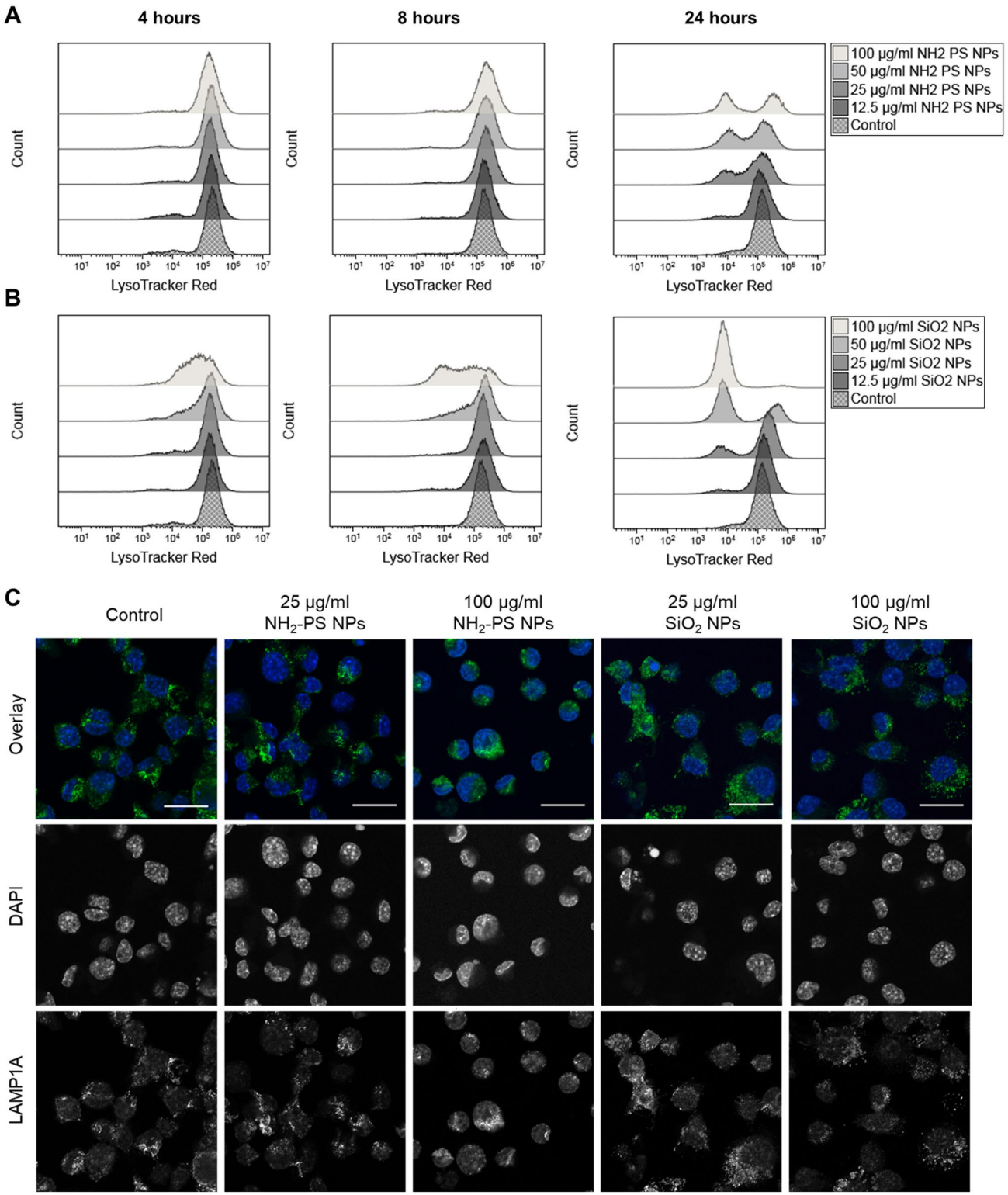

Fig. 4 Effect of NH_2-PS and SiO_2 nanoparticles on lysosomes in MPI cells. LysoTracker Red was used to monitor eventual lysosomal alterations on MPI cells exposed for the indicated times to different doses of **a** NH_2-PS and **b** SiO_2 nanoparticles. Representative examples of LysoTracker Red distributions are shown. **c** Confocal microscopy images of MPI cells after 4 h of exposure to NH_2-PS and SiO_2 nanoparticles. Green: LAMP1A stained lysosomes; blue: DAPI stained nuclei. Scale bar: 20 µm. Additional images at different exposure times are shown in Supplementary Figure S9. Overall the results suggest no evident alteration of the lysosomes after exposure to the nanoparticles (color figure online)

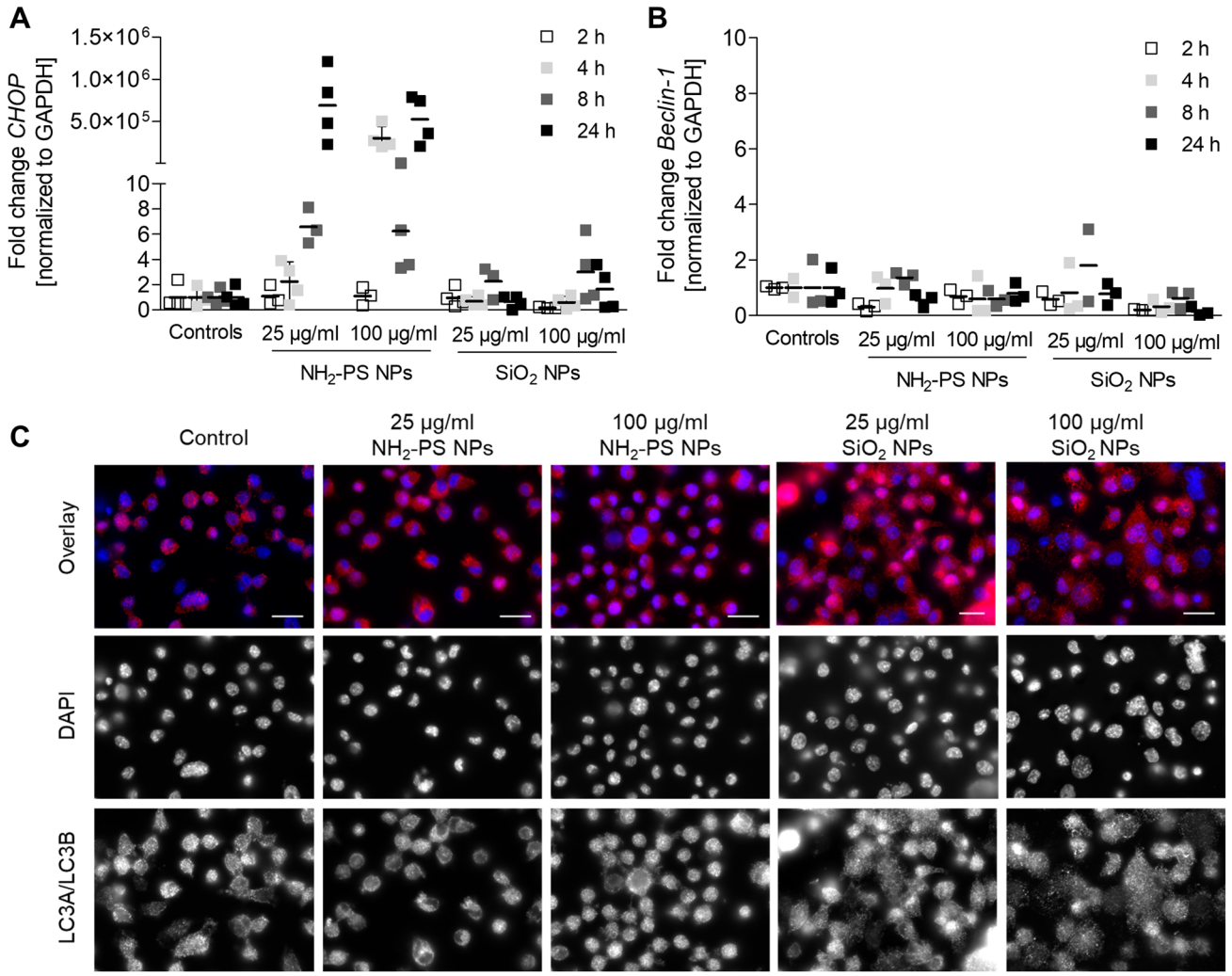

Fig. 5 Effect of NH_2-PS and SiO_2 nanoparticles on ER stress and autophagy in MPI cells. Eventual induction of ER stress (**a**) and autophagy (**b**) were monitored by measuring by RTqPCR the expression levels of, respectively, CHOP and Beclin-1 in MPI cells exposed for different times to different doses of NH_2-PS and SiO_2 nanoparticles. The results are the gene expression levels of CHOP (**a**) and Beclin-1 (**b**), normalized by the expression levels of GAPDH in the same conditions. Data are expressed as fold increase compared to untreated control cells. The results obtained in four individual experiments are shown, together with their average (indicated with a line). **c** Confocal microscopy images of MPI cells after 4 h of exposure to NH_2-PS and SiO_2 nanoparticles. Red: LC3A and LC3B staining of autophagosomal membranes; blue: DAPI-stained nuclei. Scale bar: 10 µm. Additional images at different exposure times are shown in Supplementary Figure S10. Overall CHOP results suggested activation of ER stress in cells exposed to the NH_2-PS, while Beclin-1 results and LC3 staining indicated no evident induction of autophagy in all conditions (color figure online)

followed at later times by mitochondrial ROS production and lipid peroxidation. In addition, NH_2-PS nanoparticles strongly affected mitochondrial membrane potential, with an interesting hyperpolarization observed in cells exposed to the lower doses, and—perhaps more expected—a loss of mitochondrial potential at the higher doses. Mitochondrial hyperpolarization has been observed in different cells of the immune system under stress conditions, including activated Fas signaling (Banki et al. 1999; Beltran et al. 2002) and hypoxia (Gao and Wolin 2008). Increased cellular ROS production plays a critical role in this phenomenon (Galloway and Yoon 2012). Hyperpolarization itself can induce ROS, and oxidative stress will finally impair the mitochondrial machinery causing mitochondrial depolarization, as seen here for cells exposed to the highest concentration of NH_2-PS nanoparticles. Mitochondrial hyperpolarization also enhances mitochondrial superoxide production (Murphy 2009; Pak et al. 2013), however, cells exposed to NH_2-PS nanoparticles displayed an increase in mitochondrial ROS only after 24 h of exposure and not at earlier times. It has been suggested that an initial hyperpolarization can be part of a defense mechanism to avoid apoptotic cell death. This has been supported by the observation that lymphocytes from patients with systemic lupus erythematosus have

hyperpolarized mitochondria which are resistant to apoptosis (Perl et al. 2012). Similar responses may be triggered here in cells exposed to the lower doses of the NH_2-PS nanoparticles. Further research is required to fully confirm this interpretation.

Upregulation of the gene expression of CHOP was also observed in response to NH_2-PS exposure, indicative of ER stress, which usually triggers apoptosis. However, surprisingly, regardless of the effect on mitochondrial membrane potential and indication of ER stress activation, no signs of apoptosis were detected. A possible interpretation of this series of events following NH_2-PS nanoparticle exposure is that, given the high uptake efficiency of macrophages, these nanoparticles are still toxic to cells, but without the cells having the time to activate a clear apoptotic cell death (also without signs of clear swelling in the lysosomes where nanoparticles accumulate).

On the other hand, SiO_2 nanoparticle exposure caused cell death in MPI macrophages, characterized by classic apoptotic features such as increased mitochondrial ROS, mitochondrial depolarization, caspase activation and exposure of phosphatidylserine on the cell membrane. Similar results with SiO_2 nanoparticles were obtained on RAW 364.7 macrophages (Wilhelmi et al. 2012), and other studies where alterations in inflammatory responses or cellular functions in different types of immune cells were reported (Mohamed et al. 2011; Lankoff et al. 2013; Kim et al. 2015). Similar to NH_2-PS nanoparticles exposure, also with these nanoparticles no evident lysosomal swelling was detected.

Additionally, while previous studies have observed that in some conditions exposure to silica can induce autophagy, here quantification of beclin-1 expression and LC3A/B staining did not show clear involvement of autophagy (Herd et al. 2011; Marquardt et al. 2017). A more precise analysis would be needed to fully elucidate the potential role of autophagy in the observed mechanisms of toxicity, e.g. by measuring the autophagic flux in the presence and absence of lysosomal inhibitors. Overall, these results clearly showed that the MPI cells responded in very different ways to the two selected nanoparticle models, with some interesting differences in comparison to what reported for the same materials in several other cell models. It would be important, in the future, to perform similar time-resolved studies using other macrophage models (for instance human monocyte-derived macrophages) and compare the observed responses to determine which model may provide data of higher relevance for humans.

Time-resolved approaches such as we show here can be used to determine the series of events triggered in cells following exposure to nanoparticles, and in this way determine the mechanisms involved and differences in response to different materials. Additionally, the inclusion of more representative routes for delivering the nanoparticles to the model cells, e.g., by air–liquid interface exposure (Frijns et al. 2017), could be beneficial to evaluate more realistically the interaction of nanoparticles and cells.

On a broader perspective, given the heterogeneity of tissue-specific macrophages, it would be interesting to perform similar time-resolved studies on resident macrophages of different origin, representative of the different organs in which nanoparticles distribute. For such studies, the cell-delivered dose should be determined, to ensure that realistic doses are applied, corresponding to the tissue-delivered doses observed in vivo. This could contribute to determine tissue-specific responses, and in this way to screen in vitro for potential nanoparticle outcomes at organ level. Indeed, it has been proposed that macrophages could be used for first tier screening of nanoparticle-induced effects in the different organs in which they distribute (Wiemann et al. 2016; Bhattacharya et al. 2017). On a broader context, selecting the correct cell models is well-known to be a crucial step when evaluating nanoparticle (but not only) toxicity in vitro, and clearly it is even more so, when focusing on highly specialized cells such as the macrophages. Cell lines such as the MPI alveolar-like macrophages used for this study, preserving primary cell characteristics without the usual restrictions in cell availability of primary cells, could be extremely useful models for mechanistic nanosafety investigations.

Acknowledgements SD was supported by a postdoctoral fellowship granted by the Research Foundation Flanders (FWO) and the Flemish Institute for Technological Research (VITO). The authors wish to thank Catharina Reker-Smit (University of Groningen, Groningen, The Netherlands) for assistance with the cell culturing. AMD is the recipient of a Rosalind Franklin Fellowship co-funded by the European Union and the University of Groningen. AS kindly acknowledges the University of Groningen for additional funding (Rosalind Franklin Fellowship). MPI cells were provided as a kind gift by György Fejer and Marina A. Freudenberg (Max-Planck-Institute for Immunobiology and Epigenetics, Freiburg, Germany).

Funding SD is the recipient of a postdoctoral fellowship granted by the Research Foundation Flanders (FWO) and the Flemish Institute for Technological Research (VITO) (Grant agreement 12S6517N).

Compliance with ethical standards

Conflict of interest The authors declare that they have no competing interests.

References

Aillon KL, Xie Y, El-Gendy N, Berkland CJ, Forrest ML (2009) Effects of nanomaterial physicochemical properties on in vivo toxicity. Adv Drug Deliv Rev 61(6):457–466. https://doi.org/10.1016/j.addr.2009.03.010

Andreu N, Phelan J, de Sessions PF, Cliff JM, Clark TG, Hibberd ML (2017) Primary macrophages and J774 cells respond differently to infection with Mycobacterium tuberculosis. Sci Rep 7:42225. https://doi.org/10.1038/srep42225

Auten RL, Davis JM (2009) Oxygen toxicity and reactive oxygen species: the devil is in the details. Pediatr Res 66(2):121–127. https://doi.org/10.1203/PDR.0b013e3181a9eafb

Banki K, Hutter E, Gonchoroff NJ, Perl A (1999) Elevation of mitochondrial transmembrane potential and reactive oxygen intermediate levels are early events and occur independently from activation of caspases in Fas signaling. J Immunol 162(3):1466–1479

Beltran B, Quintero M, Garcia-Zaragoza E, O'Connor E, Esplugues JV, Moncada S (2002) Inhibition of mitochondrial respiration by endogenous nitric oxide: a critical step in Fas signaling. Proc Natl Acad Sci USA 99(13):8892–8897. https://doi.org/10.1073/pnas.092259799

Bexiga MG, Varela JA, Wang F, Fenaroli F, Salvati A, Lynch I, Simpson JC, Dawson KA (2011) Cationic nanoparticles induce caspase 3-, 7- and 9-mediated cytotoxicity in a human astrocytoma cell line. Nanotoxicology 5(4):557–567. https://doi.org/10.3109/17435390.2010.539713

Bhattacharya K, Kilic G, Costa PM, Fadeel B (2017) Cytotoxicity screening and cytokine profiling of 19 nanomaterials enables hazard ranking and grouping based on inflammogenic potential. Nanotoxicology 11(6):809–826. https://doi.org/10.1080/17435390.2017.1363309

Blanco E, Hsiao A, Mann AP, Landry MG, Meric-Bernstam F, Ferrari M (2011) Nanomedicine in cancer therapy: innovative trends and prospects. Cancer Sci 102(7):1247–1252. https://doi.org/10.1111/j.1349-7006.2011.01941.x

Boraschi D, Italiani P, Palomba R, Decuzzi P, Duschl A, Fadeel B, Moghimi SM (2017) Nanoparticles and innate immunity: new perspectives on host defence. Semin Immunol 34:33–51. https://doi.org/10.1016/j.smim.2017.08.013

Bouwmeester H, Dekkers S, Noordam MY, Hagens WI, Bulder AS, de Heer C, ten Voorde SE, Wijnhoven SW, Marvin HJ, Sips AJ (2009) Review of health safety aspects of nanotechnologies in food production. Regul Toxicol Pharmacol 53(1):52–62. https://doi.org/10.1016/j.yrtph.2008.10.008

Briley-Saebo K, Bjornerud A, Grant D, Ahlstrom H, Berg T, Kindberg GM (2004) Hepatic cellular distribution and degradation of iron oxide nanoparticles following single intravenous injection in rats: implications for magnetic resonance imaging. Cell Tissue Res 316(3):315–323. https://doi.org/10.1007/s00441-004-0884-8

Buzea C, Pacheco I, Robbie K (2007) Nanomaterials and nanoparticles: sources and toxicity. Biointerphases 2(4):MR17–MR71. https://doi.org/10.1116/1.2815690

Cao Y, Long J, Liu L, He T, Jiang L, Zhao C, Li Z (2017) A review of endoplasmic reticulum (ER) stress and nanoparticle (NP) exposure. Life Sci 186:33–42. https://doi.org/10.1016/j.lfs.2017.08.003

Chanput W, Mes JJ, Wichers HJ (2014) THP-1 cell line: an in vitro cell model for immune modulation approach. Int Immunopharmacol 23(1):37–45. https://doi.org/10.1016/j.intimp.2014.08.002

De Jong WH, Borm PJA (2008) Drug delivery and nanoparticles: applications and hazards. Int J Nanomed 3(2):133–149

Deville S, Baré B, Piella J, Tirez K, Hoet P, Monopoli MP, Dawson KA, Puntes VF, Nelissen I (2016) Interaction of gold nanoparticles and nickel(II) sulfate affects dendritic cell maturation. Nanotoxicology 10(10):1395–1403. https://doi.org/10.1080/17435390.2016.1221476

Dobrovolskaia MA, Aggarwal P, Hall JB, McNeil SE (2008) Preclinical studies to understand nanoparticle interaction with the immune system and its potential effects on nanoparticle biodistribution. Mol Pharm 5(4):487–495. https://doi.org/10.1021/mp800032f

Duchen MR (2000) Mitochondria and calcium: from cell signalling to cell death. J Physiol 529(Pt 1):57–68. https://doi.org/10.1111/j.1469-7793.2000.00057.x

Fejer G, Wegner MD, Gyory I, Cohen I, Engelhard P, Voronov E, Manke T, Ruzsics Z, Dolken L, Prazeres da Costa O, Branzk N, Huber M, Prasse A, Schneider R, Apte RN, Galanos C, Freudenberg MA (2013) Nontransformed, GM-CSF-dependent macrophage lines are a unique model to study tissue macrophage functions. Proc Natl Acad Sci USA 110(24):E2191–2198. https://doi.org/10.1073/pnas.1302877110

Fejer G, Sharma S, Gyory I (2015) Self-renewing macrophages—a new line of enquiries in mononuclear phagocytes. Immunobiology 220(2):169–174. https://doi.org/10.1016/j.imbio.2014.11.005

Ferrari M (2005) Cancer nanotechnology: opportunities and challenges. Nat Rev Cancer 5(3):161–171. https://doi.org/10.1038/nrc1566

Figueiredo Borgognoni C, Kim JH, Zucolotto V, Fuchs H, Riehemann K (2018) Human macrophage responses to metal-oxide nanoparticles: a review. Artif Cells Nanomed Biotechnol. https://doi.org/10.1080/21691401.2018.1468767

Finkel T, Menazza S, Holmström KM, Parks RJ, Liu J, Sun J, Liu J, Pan X, Murphy E (2015) The ins and outs of mitochondrial calcium. Circ Res 116(11):1810. https://doi.org/10.1161/CIRCRESAHA.116.305484

Frijns E, Verstraelen S, Stoehr LC, Van Laer J, Jacobs A, Peters J, Tirez K, Boyles MSP, Geppert M, Madl P, Nelissen I, Duschl A, Himly M (2017) A novel exposure system termed NAVETTA for in vitro laminar flow electrodeposition of nanoaerosol and evaluation of immune effects in human lung reporter cells. Environ Sci Technol 51(9):5259–5269. https://doi.org/10.1021/acs.est.7b00493

Galloway CA, Yoon Y (2012) What comes first, misshape or dysfunction? The view from metabolic excess. J Gen Physiol 139(6):455. https://doi.org/10.1085/jgp.201210771

Gao Q, Wolin MS (2008) Effects of hypoxia on relationships between cytosolic and mitochondrial NAD(P)H redox and superoxide generation in coronary arterial smooth muscle. Am J Physiol Heart Circ Physiol 295(3):H978–h989. https://doi.org/10.1152/ajpheart.00316.2008

Geiser M, Casaulta M, Kupferschmid B, Schulz H, Semmler-Behnke M, Kreyling W (2008) The role of macrophages in the clearance of inhaled ultrafine titanium dioxide particles. Am J Respir Cell Mol Biol 38(3):371–376. https://doi.org/10.1165/rcmb.2007-0138OC

Gordon S, Pluddemann A, Martinez Estrada F (2014) Macrophage heterogeneity in tissues: phenotypic diversity and functions. Immunol Rev 262(1):36–55. https://doi.org/10.1111/imr.12223

Gustafson HH, Holt-Casper D, Grainger DW, Ghandehari H (2015) Nanoparticle uptake: the phagocyte problem. Nano Today 10(4):487–510. https://doi.org/10.1016/j.nantod.2015.06.006

Hansjosten I, Rapp J, Reiner L, Vatter R, Fritsch-Decker S, Peravali R, Palosaari T, Joossens E, Gerloff K, Macko P, Whelan M, Gilliland D, Ojea-Jimenez I, Monopoli MP, Rocks L, Garry D, Dawson K, Röttgermann PJF, Murschhauser A, Rädler JO, Tang SVY, Gooden P, Belinga-Desaunay M-FA, Khan AO, Briffa S, Guggenheim E, Papadiamantis A, Lynch I, Valsami-Jones E, Diabaté S, Weiss C (2018) Microscopy-based high-throughput assays enable multi-parametric analysis to assess adverse effects

of nanomaterials in various cell lines. Arch Toxicol 92(2):633–649. https://doi.org/10.1007/s00204-017-2106-7
Herd HL, Malugin A, Ghandehari H (2011) Silica nanoconstruct cellular toleration threshold in vitro. J Control Release 153(1):40–48. https://doi.org/10.1016/j.jconrel.2011.02.017
Hsia IL, Fritsch-Decker S, Leidner A, Al-Rawi M, Hug V, Diabaté S, Grage SL, Meffert M, Stoeger T, Gerthsen D, Ulrich AS, Niemeyer CM, Weiss C (2019) Biocompatibility of amine-functionalized silica nanoparticles: the role of surface coverage. Small 15(10):e1805400. https://doi.org/10.1002/smll.20180540
Kang R, Zeh HJ, Lotze MT, Tang D (2011) The Beclin 1 network regulates autophagy and apoptosis. Cell Death Different 18(4):571–580. https://doi.org/10.1038/cdd.2010.191
Kim JA, Aberg C, Salvati A, Dawson KA (2011) Role of cell cycle on the cellular uptake and dilution of nanoparticles in a cell population. Nat Nanotechnol 7(1):62–68. https://doi.org/10.1038/nnano.2011.191
Kim I-Y, Joachim E, Choi H, Kim K (2015) Toxicity of silica nanoparticles depends on size, dose, and cell type. Nanomed Nanotechnol Biol Med 11(6):1407–1416. https://doi.org/10.1016/j.nano.2015.03.004
Klein SG, Hennen J, Serchi T, Blomeke B, Gutleb AC (2011) Potential of coculture in vitro models to study inflammatory and sensitizing effects of particles on the lung. Toxicol In Vitro 25(8):1516–1534. https://doi.org/10.1016/j.tiv.2011.09.006
Klein SG, Serchi T, Hoffmann L, Blomeke B, Gutleb AC (2013) An improved 3D tetraculture system mimicking the cellular organisation at the alveolar barrier to study the potential toxic effects of particles on the lung. Part Fibre Toxicol 10:31. https://doi.org/10.1186/1743-8977-10-31
Kusaka T, Nakayama M, Nakamura K, Ishimiya M, Furusawa E, Ogasawara K (2014) Effect of silica particle size on macrophage inflammatory responses. PLoS One 9(3):e92634. https://doi.org/10.1371/journal.pone.0092634
Lam FC, Morton SW, Wyckoff J, Vu Han TL, Hwang MK, Maffa A, Balkanska-Sinclair E, Yaffe MB, Floyd SR, Hammond PT (2018) Enhanced efficacy of combined temozolomide and bromodomain inhibitor therapy for gliomas using targeted nanoparticles. Nat Commun 9(1):1991. https://doi.org/10.1038/s41467-018-04315-4
Lankoff A, Arabski M, Wegierek-Ciuk A, Kruszewski M, Lisowska H, Banasik-Nowak A, Rozga-Wijas K, Wojewodzka M, Slomkowski S (2013) Effect of surface modification of silica nanoparticles on toxicity and cellular uptake by human peripheral blood lymphocytes in vitro. Nanotoxicology 7(3):235–250. https://doi.org/10.3109/17435390.2011.649796
Lanone S, Rogerieux F, Geys J, Dupont A, Maillot-Marechal E, Boczkowski J, Lacroix G, Hoet P (2009) Comparative toxicity of 24 manufactured nanoparticles in human alveolar epithelial and macrophage cell lines. Particle Fibre Toxicol 6(1):14. https://doi.org/10.1186/1743-8977-6-14
Lesniak A, Fenaroli F, Monopoli MP, Aberg C, Dawson KA, Salvati A (2012) Effects of the presence or absence of a protein corona on silica nanoparticle uptake and impact on cells. ACS Nano 6(7):5845–5857. https://doi.org/10.1021/nn300223w
Lobatto ME, Fuster V, Fayad ZA, Mulder WJ (2011) Perspectives and opportunities for nanomedicine in the management of atherosclerosis. Nat Rev Drug Discov 10(11):835–852. https://doi.org/10.1038/nrd3578
Lunov O, Syrovets T, Loos C, Beil J, Delacher M, Tron K, Nienhaus GU, Musyanovych A, Mailander V, Landfester K, Simmet T (2011) Differential uptake of functionalized polystyrene nanoparticles by human macrophages and a monocytic cell line. ACS Nano 5(3):1657–1669. https://doi.org/10.1021/nn2000756
Lv H, Zhang S, Wang B, Cui S, Yan J (2006) Toxicity of cationic lipids and cationic polymers in gene delivery. J Control Release 114(1):100–109. https://doi.org/10.1016/j.jconrel.2006.04.014
Maler MD, Nielsen PJ, Stichling N, Cohen I, Ruzsics Z, Wood C, Engelhard P, Suomalainen M, Gyory I, Huber M, Muller-Quernheim J, Schamel WWA, Gordon S, Jakob T, Martin SF, Jahnen-Dechent W, Greber UF, Freudenberg MA, Fejer G (2017) Key role of the scavenger receptor MARCO in mediating adenovirus infection and subsequent innate responses of macrophages. MBio. https://doi.org/10.1128/mBio.00670-17
Mamo T, Moseman EA, Kolishetti N, Salvador-Morales C, Shi J, Kuritzkes DR, Langer R, von Andrian U, Farokhzad OC (2010) Emerging nanotechnology approaches for HIV/AIDS treatment and prevention. Nanomedicine (London) 5(2):269–285. https://doi.org/10.2217/nnm.10.1
Marquardt C, Fritsch-Decker S, Al-Rawi M, Diabate S, Weiss C (2017) Autophagy induced by silica nanoparticles protects RAW264.7 macrophages from cell death. Toxicology 379:40–47. https://doi.org/10.1016/j.tox.2017.01.019
Mohamed BM, Verma NK, Prina-Mello A, Williams Y, Davies AM, Bakos G, Tormey L, Edwards C, Hanrahan J, Salvati A, Lynch I, Dawson K, Kelleher D, Volkov Y (2011) Activation of stress-related signalling pathway in human cells upon SiO2 nanoparticles exposure as an early indicator of cytotoxicity. J Nanobiotechnol 9:29. https://doi.org/10.1186/1477-3155-9-29
Murphy MP (2009) How mitochondria produce reactive oxygen species. Biochem J 417(1):1. https://doi.org/10.1042/BJ20081386
Neitemeier S, Jelinek A, Laino V, Hoffmann L, Eisenbach I, Eying R, Ganjam GK, Dolga AM, Oppermann S, Culmsee C (2017) BID links ferroptosis to mitochondrial cell death pathways. Redox Biol 12:558–570. https://doi.org/10.1016/j.redox.2017.03.007
Oberdorster G (2010) Safety assessment for nanotechnology and nanomedicine: concepts of nanotoxicology. J Intern Med 267(1):89–105. https://doi.org/10.1111/j.1365-2796.2009.02187.x
Owens DE 3rd, Peppas NA (2006) Opsonization, biodistribution, and pharmacokinetics of polymeric nanoparticles. Int J Pharm 307(1):93–102. https://doi.org/10.1016/j.ijpharm.2005.10.010
Pak O, Sommer N, Hoeres T, Bakr A, Waisbrod S, Sydykov A, Haag D, Esfandiary A, Kojonazarov B, Veit F, Fuchs B, Weisel FC, Hecker M, Schermuly RT, Grimminger F, Ghofrani HA, Seeger W, Weissmann N (2013) Mitochondrial hyperpolarization in pulmonary vascular remodeling. Mitochondrial uncoupling protein deficiency as disease model. Am J Respir Cell Mol Biol 49(3):358–367. https://doi.org/10.1165/rcmb.2012-0361OC
Pan C, Kumar C, Bohl S, Klingmueller U, Mann M (2009) Comparative proteomic phenotyping of cell lines and primary cells to assess preservation of cell type-specific functions. Mol Cell Proteomics 8(3):443–450. https://doi.org/10.1074/mcp.M800258-MCP200
Park E-J, Roh J, Kim Y, Choi K (2011) A single instillation of amorphous silica nanoparticles induced inflammatory responses and tissue damage until day 28 after exposure. J Health Sci 57(1):60–71. https://doi.org/10.1248/jhs.57.60
Perl A, Hanczko R, Doherty E (2012) Assessment of mitochondrial dysfunction in lymphocytes of patients with systemic lupus erythematosus. Methods Mol Biol 900:61–89. https://doi.org/10.1007/978-1-60761-720-4_4
Pouliquen D, Le Jeune JJ, Perdrisot R, Ermias A, Jallet P (1991) Iron oxide nanoparticles for use as an MRI contrast agent: pharmacokinetics and metabolism. Magn Reson Imaging 9(3):275–283. https://doi.org/10.1016/0730-725X(91)90412-F
Rivera Gil P, Oberdorster G, Elder A, Puntes V, Parak WJ (2010) Correlating physico-chemical with toxicological properties of nanoparticles: the present and the future. ACS Nano 4(10):5527–5531. https://doi.org/10.1021/nn1025687
Ruenraroengsak P, Novak P, Berhanu D, Thorley AJ, Valsami-Jones E, Gorelik J, Korchev YE, Tetley TD (2012) Respiratory epithelial cytotoxicity and membrane damage (holes) caused by

amine-modified nanoparticles. Nanotoxicology 6(1):94–108. https://doi.org/10.3109/17435390.2011.558643

Schlinkert P, Casals E, Boyles M, Tischler U, Hornig E, Tran N, Zhao J, Himly M, Riediker M, Oostingh GJ, Puntes V, Duschl A (2015) The oxidative potential of differently charged silver and gold nanoparticles on three human lung epithelial cell types. J Nanobiotechnol 13:1. https://doi.org/10.1186/s12951-014-0062-4

Shapero K, Fenaroli F, Lynch I, Cottell DC, Salvati A, Dawson KA (2011) Time and space resolved uptake study of silica nanoparticles by human cells. Mol BioSyst 7(2):371–378. https://doi.org/10.1039/c0mb00109k

Soenen SJ, Rivera-Gil P, Montenegro J-M, Parak WJ, De Smedt SC, Braeckmans K (2011) Cellular toxicity of inorganic nanoparticles: common aspects and guidelines for improved nanotoxicity evaluation. Nano Today 6(5):446–465. https://doi.org/10.1016/j.nantod.2011.08.001

Stichling N, Suomalainen M, Flatt JW, Schmid M, Pacesa M, Hemmi S, Jungraithmayr W, Maler MD, Freudenberg MA, Plückthun A, May T, Köster M, Fejer G, Greber UF (2018) Lung macrophage scavenger receptor SR-A6 (MARCO) is an adenovirus type-specific virus entry receptor. PLoS Pathog 14(3):e1006914. https://doi.org/10.1371/journal.ppat.1006914

Tait SWG, Green DR (2013) Mitochondrial Regulation of Cell Death. Cold Spring Harbor Perspect Biol 5(9):a008706. https://doi.org/10.1101/cshperspect.a008706

Tavares AJ, Poon W, Zhang YN, Dai Q, Besla R, Ding D, Ouyang B, Li A, Chen J, Zheng G, Robbins C, Chan WCW (2017) Effect of removing Kupffer cells on nanoparticle tumor delivery. Proc Natl Acad Sci USA 114(51):E10871–e10880. https://doi.org/10.1073/pnas.1713390114

Thomas DG, Smith JN, Thrall BD, Baer DR, Jolley H, Munusamy P, Kodali V, Demokritou P, Cohen J, Teeguarden JG (2018) ISD3: a particokinetic model for predicting the combined effects of particle sedimentation, diffusion and dissolution on cellular dosimetry for in vitro systems. Part Fibre Toxicol 15:6. https://doi.org/10.1186/s12989-018-0243-7

Thornton C, Hagberg H (2015) Role of mitochondria in apoptotic and necroptotic cell death in the developing brain. Clin Chim Acta 451:35–38. https://doi.org/10.1016/j.cca.2015.01.026

Walkey CD, Olsen JB, Guo H, Emili A, Chan WC (2012) Nanoparticle size and surface chemistry determine serum protein adsorption and macrophage uptake. J Am Chem Soc 134(4):2139–2147. https://doi.org/10.1021/ja2084338

Wang F, Bexiga MG, Anguissola S, Boya P, Simpson JC, Salvati A, Dawson KA (2013a) Time resolved study of cell death mechanisms induced by amine-modified polystyrene nanoparticles. Nanoscale 5(22):10868–10876. https://doi.org/10.1039/c3nr03249c

Wang F, Yu L, Monopoli MP, Sandin P, Mahon E, Salvati A, Dawson KA (2013b) The biomolecular corona is retained during nanoparticle uptake and protects the cells from the damage induced by cationic nanoparticles until degraded in the lysosomes. Nanomedicine 9(8):1159–1168. https://doi.org/10.1016/j.nano.2013.04.010

Wang F, Salvati A, Boya P (2018) Lysosome-dependent cell death and deregulated autophagy induced by amine-modified polystyrene nanoparticles. Open Biol. https://doi.org/10.1098/rsob.170271

Wiemann M, Vennemann A, Sauer UG, Wiench K, Ma-Hock L, Landsiedel R (2016) An in vitro alveolar macrophage assay for predicting the short-term inhalation toxicity of nanomaterials. J Nanobiotechnol 14:16. https://doi.org/10.1186/s12951-016-0164-2

Wilhelm S, Tavares AJ, Dai Q, Ohta S, Audet J, Dvorak HF, Chan WCW (2016) Analysis of nanoparticle delivery to tumours. Nat Rev Mater 1:16014. https://doi.org/10.1038/natrevmats.2016.14

Wilhelmi V, Fischer U, van Berlo D, Schulze-Osthoff K, Schins RP, Albrecht C (2012) Evaluation of apoptosis induced by nanoparticles and fine particles in RAW 264.7 macrophages: facts and artefacts. Toxicol In Vitro 26(2):323–334. https://doi.org/10.1016/j.tiv.2011.12.006

Wohlleben W, Driessen MD, Raesch S, Schaefer UF, Schulze C, Vacano B, Vennemann A, Wiemann M, Ruge CA, Platsch H, Mues S, Ossig R, Tomm JM, Schnekenburger J, Kuhlbusch TA, Luch A, Lehr CM, Haase A (2016) Influence of agglomeration and specific lung lining lipid/protein interaction on short-term inhalation toxicity. Nanotoxicology 10(7):970–980. https://doi.org/10.3109/17435390.2016.1155671

Xia T, Kovochich M, Liong M, Zink JI, Nel AE (2008) Cationic polystyrene nanosphere toxicity depends on cell-specific endocytic and mitochondrial injury pathways. ACS Nano 2(1):85–96. https://doi.org/10.1021/nn700256c

Xia T, Li N, Nel AE (2009) Potential health impact of nanoparticles. Annu Rev Public Health 30:137–150. https://doi.org/10.1146/annurev.publhealth.031308.100155

Ye D, Bramini M, Hristov DR, Wan S, Salvati A, Aberg C, Dawson KA (2017) Low uptake of silica nanoparticles in Caco-2 intestinal epithelial barriers. Beilstein J Nanotechnol 8:1396–1406. https://doi.org/10.3762/bjnano.8.141